# Space- and Time-Resolved Interferometry of Plasma-Filled Rod-Pinch Diodes *

**David M. Ponce †‡, David Phipps §, David D. Hinshelwood, and B. V. Weber**

*Plasma Physics Division, Naval Research Laboratory*
*Washington, D.C. 20375 USA*

*Abstract*

This paper presents results from interferometric diagnosis of plasma dynamics in a plasma-filled rod-pinch diode (PFRP) on GAMBLE II at NRL, with diode voltages and currents of 1 MV and 600 kA respectively. A high sensitivity interferometer shows the time history of the prefill plasma moving past the anode tip propelled by a $\vec{J} \times \vec{B}$ snowplow. Images from a 2-D holographic interferometer show the gun plasma MHD evolution and show the anode tip explode after the start of the x-ray pulse. The results of these studies will be used as experimental benchmarks in the theoretical studies of the PFRP.

## I. INTRODUCTION

Pulsed radiography requires an intense, small spot size x-ray source. It has been demonstrated that high x-ray yield (several R @ 1 m) with a small spot size ($\lesssim$ 1 mm) can be achieved with a rod-pinch diode (RP)[1, 2]. Although the RP is suitable for some radiographic applications, higher dose is desired without increasing source size. An enhanced version of the RP is the plasma-filled rod-pinch diode (PFRP). The PFRP has the same configuration as the RP with the addition of a plasma produced by a set of plasma cable guns. This gun plasma provides an initial electrical connection between the PFRP electrodes. Figure 1 shows a PFRP configuration used in GAMBLE II where the anode is a 10 cm long tungsten rod with 1 mm diameter, tapered to a point over the last 10 mm. The anode tip protrudes $\sim 3.8$ cm from the cathode plane. The PFRP electrical characteristics, x-ray yield, radiographic spot size, and line-pair resolution are described in references [3, 4]. Typical GAMBLE II PFRP operating parameters are (0.45 MV, 770 kA, 0.5 Ω) to (1.8 MV, 260 kA, 7 Ω). The diode impedance is zero initially (for $\sim 40$ ns from generator firing), then it transitions to a high impedance phase when x-rays are produced yielding 20 rad @ 1 m through 3 mm aluminum. The plasma fill provided by the plasma guns can be varied by either repositioning the guns with respect to the anode or by adding delay in the trigger chain. The PFRP impedance decreases as the fill density increases. Proper plasma fill-generator timing synchronization provides for most of the energy to be deposited at the tip of the anode during the high impedance phase.

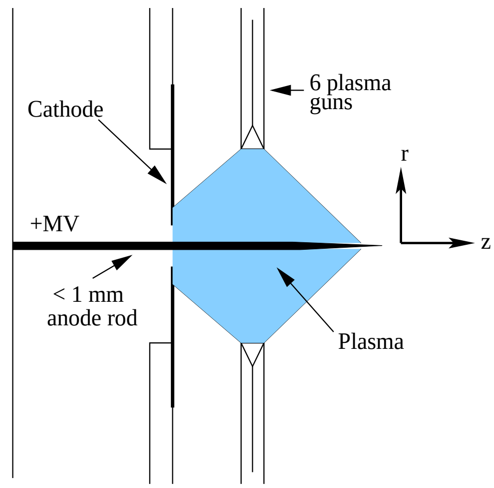


Figure 1: The PFRP consists of a tapered tungsten anode rod 1 mm $\phi$ surrounded by six plasma guns. Shown is a side view of the PFRP configuration used on GAMBLE II to diagnose plasma dynamics.

This paper shows results from a set of interferometric measurements done on the PFRP at GAMBLE II. Section II describes the diagnostics used to measure the plasmas in the PFRP and Section III is a discussion of a simple phenomenological model that explains the observed plasma dynamics.

## II. DIAGNOSTICS

Two interferometric diagnostics are used to investigate the plasma dynamics in the PFRP diode. The first is a 2-D holographic interferometer using a 150 ps pulse Nd:YAG doubled laser ($\lambda = 532$ nm) that cre-

*Work supported the Defense Threat Reduction Agency and the U.S. Office of Naval Research.

†National Research Council Research Associate at NRL
‡author's e-mail: dmponce@suzie.nrl.navy.mil
§Titan/Jaycor, McLean, VA 22102

<table>
<tr><td colspan="3">Report Documentation Page</td><td colspan="2">Form Approved<br>OMB No. 0704-0188</td></tr>
<tr><td colspan="5">Public reporting burden for the collection of information is estimated to average 1 hour per response, including the time for reviewing instructions, searching existing data sources, gathering and maintaining the data needed, and completing and reviewing the collection of information. Send comments regarding this burden estimate or any other aspect of this collection of information, including suggestions for reducing this burden, to Washington Headquarters Services, Directorate for Information Operations and Reports, 1215 Jefferson Davis Highway, Suite 1204, Arlington VA 22202-4302. Respondents should be aware that notwithstanding any other provision of law, no person shall be subject to a penalty for failing to comply with a collection of information if it does not display a currently valid OMB control number.</td></tr>
<tr><td>1. REPORT DATE<br>JUN 2003</td><td colspan="2">2. REPORT TYPE<br>N/A</td><td colspan="2">3. DATES COVERED<br>-</td></tr>
<tr><td colspan="3">4. TITLE AND SUBTITLE<br>Space- and Time-Resolved Interferometry of Plasma-Filled Rod-Pinch Diodes</td><td colspan="2">5a. CONTRACT NUMBER<br>5b. GRANT NUMBER<br>5c. PROGRAM ELEMENT NUMBER</td></tr>
<tr><td colspan="3">6. AUTHOR(S)</td><td colspan="2">5d. PROJECT NUMBER<br>5e. TASK NUMBER<br>5f. WORK UNIT NUMBER</td></tr>
<tr><td colspan="3">7. PERFORMING ORGANIZATION NAME(S) AND ADDRESS(ES)<br>Plasma Physics Division, Naval Research Laboratory Washington, D.C. 20375 USA</td><td colspan="2">8. PERFORMING ORGANIZATION REPORT NUMBER</td></tr>
<tr><td colspan="3">9. SPONSORING/MONITORING AGENCY NAME(S) AND ADDRESS(ES)</td><td colspan="2">10. SPONSOR/MONITOR’S ACRONYM(S)<br>11. SPONSOR/MONITOR’S REPORT NUMBER(S)</td></tr>
<tr><td colspan="5">12. DISTRIBUTION/AVAILABILITY STATEMENT<br>Approved for public release, distribution unlimited</td></tr>
<tr><td colspan="5">13. SUPPLEMENTARY NOTES<br>See also ADM002371. 2013 IEEE Pulsed Power Conference, Digest of Technical Papers 1976-2013, and Abstracts of the 2013 IEEE International Conference on Plasma Science. IEEE International Pulsed Power Conference (19th). Held in San Francisco, CA on 16-21 June 2013. U.S. Government or Federal Purpose Rights License, The original document contains color images.</td></tr>
<tr><td colspan="5">14. ABSTRACT<br>This paper presents results from interferometric diagnosis of plasma dynamics in a plasma-filled rodpinch diode (PFRP) on GAMBLE II at NRL, with diode voltages and currents of 1MV and 600 kA respectively. A high sensitivity interferometer shows the time history of the prefill plasma moving past the anode tip propelled by a ~ J £ ~B snowplow. Images from a 2-D holographic interferometer show the gun plasma MHD evolution and show the anode tip explode after the start of the x-ray pulse. The results of these studies will be used as experimental benchmarks in the theoretical studies of the PFRP.</td></tr>
<tr><td colspan="5">15. SUBJECT TERMS</td></tr>
<tr><td colspan="3">16. SECURITY CLASSIFICATION OF:</td><td rowspan="2">17. LIMITATION OF ABSTRACT<br>SAR</td><td rowspan="2">18. NUMBER OF PAGES<br>4</td><td rowspan="2">19a. NAME OF RESPONSIBLE PERSON</td></tr>
<tr><td>a. REPORT<br>unclassified</td><td>b. ABSTRACT<br>unclassified</td><td>c. THIS PAGE<br>unclassified</td></tr>
</table>

ates side-on holographic images at two times with a variable optical delay of 5 ns to 50 ns [5]. The holographic plate captures both intensity and phase information with a time resolution given by the scene beam pulse width and spatial resolution mostly given by the holographic plate emulsion and image magnification. Spatial resolution in our case is in the submillimeter range. Once the holographic plate is exposed and developed, the stored data is used to reconstruct the original scene beam and perform post-experiment analysis such as conventional interferometry, schlieren shadowgraphy, shearing interferometry and so on.

The second technique is a two-color, high-sensitivity interferometer, using $\lambda = 532$ nm and $\lambda = 1064$ nm in cw mode for time-dependent line-density measurements [6]. It is capable of measuring line-integrated plasma densities $\gtrsim 10^{12}\,\mathrm{cm}^{-2}$ with $\lesssim 1$ mm spatial resolution. The PFRP was probed with the scene beam line-of-sight perpendicular to the anode rod.

In the following section we present PFRP results from the holographic and the high sensitivity interferometers and a simple model based on the measurements.

## III. PHENOMENOLOGY

In the PFRP the initial effect of the gun plasma is to provide a conduction path from the cathode to the anode, making the impedance of the diode initially very small. The diode maximum impedance is a function of the initial plasma density. This plasma density is controlled by adjusting the relative timing between the plasma gun current and the generator, or by changing the gun position relative to the anode. Figure 2 shows the time history of the plasma gun current waveform and the gun plasma line-integrated density at $r = z = 3$ mm where the origin is at the anode tip. The time $t = 0$ corresponds to GAMBLE II firing for shot 8364 in particular. One can choose, as a PFRP initial condition, a line-integrated plasma density of about $\sim 10^{14}\,\mathrm{cm}^{-2}$ to about $\sim 10^{16}\,\mathrm{cm}^{-2}$. For example, for shots 8325, 8338, and 8341, GAMBLE II fired at $\sim -0.5\,\mu$s in Figure 2, which corresponds to a plasma line-integrated density of $\sim 2 \times 10^{15}\,\mathrm{cm}^{-2}$ in the neighborhood of the rod tip. This is to be compared to $\sim 5 \times 10^{15}\,\mathrm{cm}^{-2}$ for shot 8364.

When the generator fires the current increases rapidly due to the low initial impedance of the diode. Figure 3 shows the current and x-ray pulse waveforms for shot 8338 on GAMBLE II. The plasma is snowplowed toward the tip of the anode rod by the $\vec{J} \times \vec{B}$ force. Once the current carrying plasma reaches the tip, an A-K gap is formed increasing the diode impedance. Due to this gap, the electronic energy deposition mostly occurs at the tip, hence producing a very intense x-ray burst [3, 4].

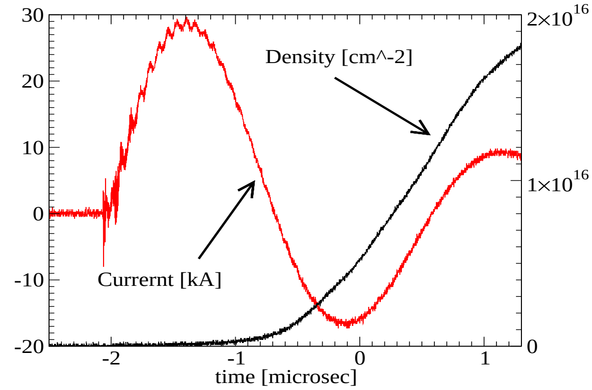


Figure 2: Plasma gun current waveform and line-integrated density as a function of time. Plasma measured at $r = z = 3$ mm from the anode tip with the

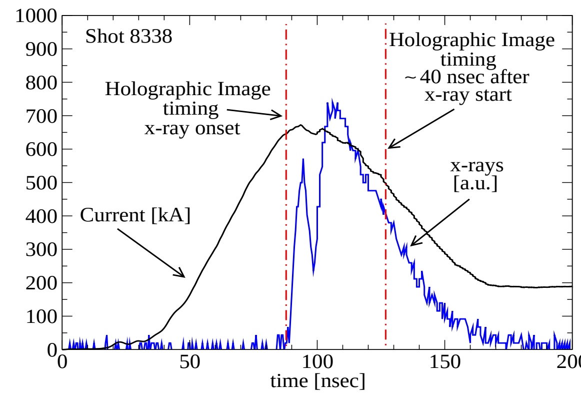


Figure 3: PFRP current waveform for shot 8338. Also shown is the x-ray signal (a.u.) and the timing at which the images of figure 4b) and figure 4c) were taken.

Figure 4 shows a series of pictures taken with the holographic interferometer showing the evolution of the PFRP plasmas. Figure 4a) is a shadowgraph image 20 ns before the start of the x-rays (and 50 ns after the start of the generator current) showing the gun plasma being snowplowed toward the anode tip by the $\vec{J} \times \vec{B}$ force, where there is about 0.5 MA flowing through the plasma to the rod at this time. The vertical lines in Figure 3 show the times when Figure 4b) and Figure 4c) where taken relative to the x-ray pulse and the generator current. Figure 4b) is a shadowgraph at the x-ray onset. Note that the high density snowplow has dissipated and the anode rod shows no evidence of physical change even though the current has increased to 630 kA in 50 ns. Figure 4c), shows the anode tip exploding at 40 ns after the start of the x-rays. There is significant plasma expansion at the rod tip after the start of the x-ray pulse. Most of the energy deposition occurs at the anode tip, relative to the tapered stalk. The characteristics of the exploding tip can be related to the intense electron deposition there.

All of the above suggest an MHD dominated regime during the initial low impedance phase up to the time when the A-K gap appears. Then the intense electron beam deposits most of its energy at the tip producing bremsstrahlung as well as rapid heating that promotes the tip hydrodynamic expansion.

In order to be able to compare experiment with theory, more quantitative data are required. Figure 5 shows an interferogram at 110 ns after the start of the x-ray pulse. The letters a) and b) in the figure mark two regions where data analysis was done. From Figure 5 we extract the line-integrated plasma density profile in the 10 mm axial region a). These results are shown in Figure 7. Figure 5 position b) shows the location in which the plasma was probed with the high sensitivity interferometer. Results are shown in Figure 6.

From Figure 6 we see the time evolution of the gun plasma at 3 mm radially and 3 mm axially from the tip of the rod. The plasma during the PFRP shot is compared with the plasma produced by the guns alone and referenced in time to the x-ray pulse. The gun plasma density increases by the snowplow action at the onset of the x-rays. We speculate that the measured plasma density is in its majority that of the guns and not from the rod since there is no electrode expansion before any x-rays appear. Tip hydro-expansion occurs after the start of the x-ray pulse, so any increase of plasma density 3 mm away from the tip of the rod has to be gun plasma swept by the snowplow. The electrode material behind the schlieren boundary reaches $r = z = 3\,\mathrm{mm}$ at $t = 110\,\mathrm{ns}$ from x-ray on-set, depicted by the vertical line in Figure 6. The maximum line density measured with the high-sensitivity interferometer was about $1.8 \times 10^{16}\,\mathrm{cm}^{-2}$ which is the interferometer's upper measuring bound caused by beam refraction.

Figure 7 shows the line-integrated density in the region $r = 0$, $3\,\mathrm{mm} \leq z \leq 10\,\mathrm{mm}$ at $t = 110\,\mathrm{ns}$. The vertical line indicates where the schlieren boundary of Figure 5 is located. There is no density data for $r < 3\,\mathrm{mm}$, where the density is dominated by the exploded high-Z rod material in that region. For $r > 3\,\mathrm{mm}$ the plasma from the cable gun is swept away by the high density material of the exploding tip and the shock front raises the line-integrated plasma density to a value of approximately $4.0 \times 10^{18}\,\mathrm{cm}^{-2}$. The line-integrated plasma density then tapers off to about $2.6 \times 10^{17}\,\mathrm{cm}^{-2}$.

One could, in principle, extrapolate this density rise in Figure 6 with the aid of Figure 7 and say that the density reaches the values on the order of $10^{18}\,\mathrm{cm}^{-2}$ at the time when the schlieren boundary appears at position b) in Figure 5, 110 ns after the start of the x-ray pulse.

The physics and dynamics of the PFRP anode tip

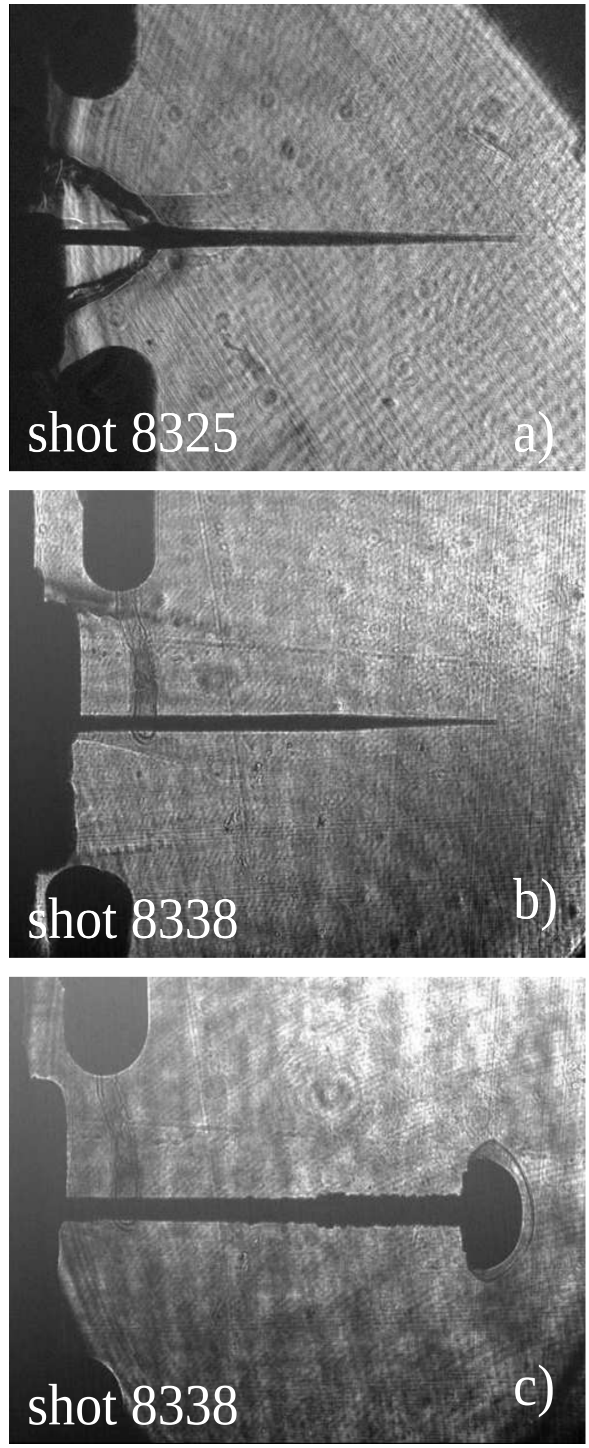


Figure 4: Series of sequential images depicting the different stages of the PFRP: a).- Plasma snowplow 20 ns before x-ray onset, b).- Onset of x-ray emission, c).- Hydrodynamic expansion of tip material at 40 ns after start of x-rays. Rod diameter at stalk is 1 mm.

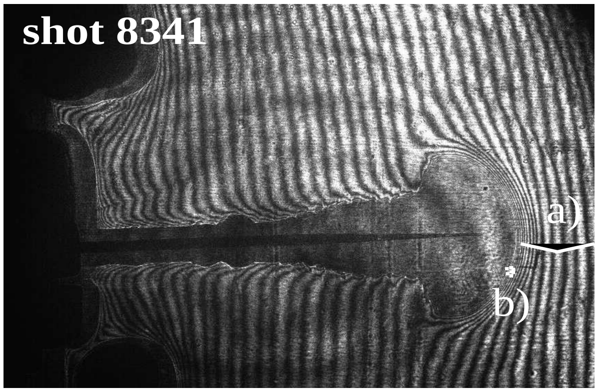


Figure 5: Reconstructed interferogram and superposed rod shadow. Hydrodynamic expansion of tip correspond to $t = 110\,\text{ns}$ from x-ray onset. a) Region ($r = 0$, $3\,\text{mm} \leq z \leq 10\,\text{mm}$) where integrated line density of Figure 7 was computed, b) Location where data of Figure 6 was collected.

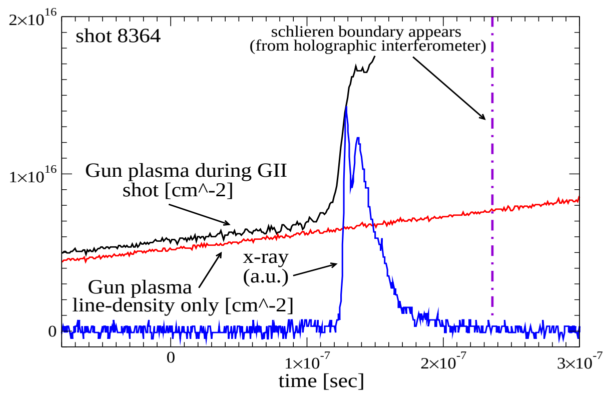


Figure 6: Line integrated plasma density as a function of time for shot 8364 at $r = z = 3\,\text{mm}$. The origin is located at the rod tip.

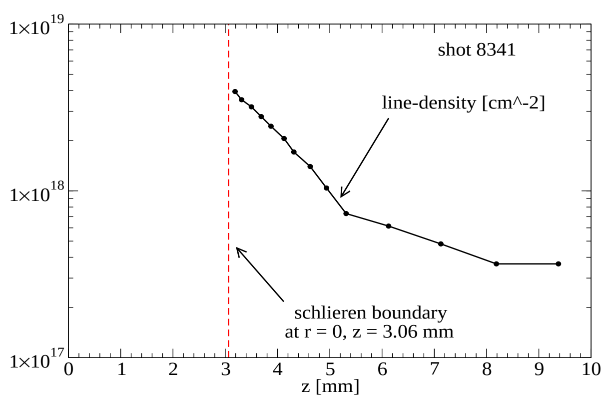


Figure 7: Line-integrated plasma density as a function of axial distance at $t = 110\,\text{ns}$ from x-ray on-set. The origin is located at the rod tip.

expansion are modeled with zero-and one-dimesional self-similar codes in reference [7]. The data presented here provide the experimental benchmarks for these theoretical models.

## IV. CONCLUSION

Two different interferometric measurements have been performed on the GAMBLE II PFRP. The space and time resolved data supports a simple phenomenological model of the PFRP. It is observed that the PFRP low impedance phase is MHD dominated. During x-ray emission there is intense beam deposition at the anode's tip that leads to hydrodynamic expansion of the tip material. This study presents the initial attempt to more fully understand PFRP physics. More interferometric measurements are planned to map the evolution of the injected plasma and the electrode plasma for different PFRP conditions. Measurement of the tip plasma temperature, estimated between 50 eV and 100 eV, is also of interest. X-ray diodes (XRDs) will be used for this purpose.

## V. REFERENCES

[1] G. Cooperstein *et al.*, "Theoretical modeling and experimental characterization of a rod-pinch diode," *Phys. Plasmas*, vol. 8, pp. 4618–4636, October 2001.

[2] R. J. Commisso *et al.*, "Experimental evaluation of a megavolt rod pinch diode as a radiography source," *IEEE Trans. Plasma Sci.*, vol. 30, pp. 338–350, 2002.

[3] B. V. Weber *et al.*, "Plasma-filled rod-pinch diode experiment on GAMBLE II," in *Proceedings of the 13th Inter. Pulsed Power Conf.*, p. 462, 2001.

[4] B. V. Weber *et al.*, "The plasma-filled rod-pinch diode: a new technique to concentrate MeV electron beams to ultra-high power and energy densities," in *AIP Conf. Proc.*, vol. 650, pp. 191–194, 2002.

[5] Installed at NRL by J. Moschella and C. Vidoli, HY-Tech Research Corp.

[6] B. V. Weber and S. F. Fulghum, "A high sensitivity two-color interferometer for pulsed power plasmas," *Rev. Sci. Instrum.*, vol. 68, no. 2, pp. 1227–1232, 1997.

[7] D. Mosher *et al.* these proceedings.